Plant Stress 10 (2023) 100250

Contents lists available at ScienceDirect

Plant Stress

journal homepage: www.sciencedirect.com/journal/plant-stress

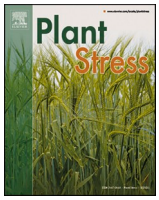

Suboptimal zinc supply affects the *S*-nitrosoglutathione reductase enzyme and nitric oxide signaling in Arabidopsis

Dóra Oláh [a,b], Selahattin Kondak [a,b], Árpád Molnár [a], Oluwatosin Peace Adedokun [a], Zalán Czékus [a], Katalin Gémes [a,c], Gábor Galbács [d], Zsuzsanna Kolbert [a,*]

[a] Department of Plant Biology, University of Szeged, Közép fasor 52., 6726 Szeged, Hungary
[b] Doctoral School of Biology, Faculty of Science and Informatics, University of Szeged, Közép fasor 52., 6726 Szeged, Hungary
[c] Institute of Plant Biology, Biological Research Centre, Hungarian Academy of Sciences, Temesvári krt. 62., 6726 Szeged, Hungary
[d] Department of Inorganic, Organic and Analytical Chemistry, University of Szeged, Dóm tér 7-8., 6720 Szeged, Hungary

ARTICLE INFO

Keywords:
Arabidopsis thaliana
Nitric oxide
S-nitrosoglutathione reductase
Suboptimal zinc supply

ABSTRACT

The *S*-nitrosoglutathione reductase (GSNOR), a key regulator of nitric oxide (NO) signaling, requires zinc (Zn) cofactors for its catalytic activity. Possible changes in GSNOR function and NO signaling due to limited Zn supply and participation of GSNOR in response to Zn deficiency have not yet been examined. The wild-type *Arabidopsis thaliana* seedlings (Col-0) and the overproducer of GSNOR (*35S::FLAG-GSNOR1*) were grown in agar medium supplemented with 15 μM (full Zn), 1.5 μM (Zn/10) and 0 μM (Zn0) zinc sulfate. Limited availability of Zn in the nutrient medium during the experimental period resulted in a significantly reduced Zn content in the roots and shoots of Arabidopsis and altered the expression of Zn deficiency marker genes; however, the Zn content did not reflect Zn deficiency in the seedlings. GSNOR has no effect on the Zn limitation-induced reduction in the *in planta* Zn content. Suboptimal Zn supply results in a smaller but more active GSNOR protein pool in Col-0 *A. thaliana*. In *35S::FLAG-GSNOR1,* overproduction possibly compensates for the negative effects of reduced Zn supply, resulting in unchanged GSNOR expression, protein abundance, and activity. Suboptimal Zn supply alters NO but did not modify peroxynitrite and hydrogen peroxide levels and exerts a pronitrant effect in the plant proteome. Overall, this is the first report to show that limited Zn supply affects the GSNOR enzyme at the gene and protein levels but not at the activity level and modifies reactive species levels and physiological nitroproteome in Arabidopsis.

1. Introduction

Low levels of zinc (Zn) in soils are a prevalent problem worldwide, as almost 30% of agricultural soils are affected by Zn deficiency in the world (Alloway, 2008; Das et al., 2019). Zinc is a crucial micronutrient that is necessary for the survival and proper functioning of all living organisms, including plants. Zinc activates more than 300 plant enzymes that participate in essential biological processes such as carbohydrate metabolism, preserving the structure of cell membranes, protein synthesis, regulation of auxin synthesis, and pollen formation (Natasha et al., 2022). Zinc deficiency in plants occurs mainly due to low Zn solubility and/or high Zn binding in the soils. At the cellular level, Zn limitation induces the overproduction of reactive oxygen species (ROS) such as superoxide anion ($O_2^{\cdot-}$) and hydrogen peroxide (H_2O_2) primarily due to down-regulation of antioxidant enzymes (Cakmak, 2000; Molnár et al., 2022). Recently, reactive nitrogen species (RNS)-associated signaling has also been linked to suboptimal Zn supply in *Brassica napus* (Molnár et al., 2022; Kondak et al., 2022). Reactive nitrogen species including nitric oxide (NO), *S*-nitrosoglutathione (GSNO), and peroxynitrite ($ONOO^-$) regulate various phytophysiological processes mainly through post-translational modifications (PTMs) such as *S*-nitrosation and tyrosine nitration. Tyrosine nitration occurs when a nitro moiety (NO_2) binds to the aromatic ring of a tyrosine, resulting in the formation of *3*-nitrotyrosine in the target protein (Gow et al., 2004; Kolbert et al., 2017). Tyrosine nitration is mediated primarily by $ONOO^-$ formed in the reaction between NO and $O_2^{\cdot-}$ (Szabó et al., 2007). *S*-nitrosoglutathione is a low molecular weight *S*-nitrosothiol (SNO) that is generated by the *S*-nitrosation of a cysteine (Cys) moiety in glutathione (GSH) (Corpas et al., 2013). The control of GSNO levels is achieved by nonenzymatic and enzymatic degradation. The enzyme GSNO reductase

* Corresponding author.
E-mail address: ordogne.kolbert.zsuzsanna@szte.hu (Z. Kolbert).

https://doi.org/10.1016/j.stress.2023.100250
Received 5 July 2023; Received in revised form 10 September 2023; Accepted 6 October 2023
Available online 8 October 2023

(GSNOR) belonging to the class III alcohol dehydrogenase family (EC 1.1.1.1) catalyzes the conversion of GSNO to glutathione disulfide (GSSG) and ammonia (NH_3) thus is responsible for controlling the enzymatic turnover of GSNO (Sakamoto et al., 2002; Jahnová et al., 2019). By controlling the concentration of SNOs in plants, GSNOR indirectly regulates nitrosative signaling and is therefore an important regulatory enzyme during stress responses. GSNOR is a highly conserved homodimeric enzyme present in mammals, yeast, and plants and it contains two Zn atoms as cofactors *per* subunit. The enzyme is rich in Cys, which coordinate Zn atoms with structural and catalytic functions (Lindermayr, 2018). As a result of the Zn requirement of GSNOR, it is attractive to hypothesize that inadequate Zn supply may influence enzyme function and consequently NO signaling. Moreover, GSNOR-controlled NO signaling is supposed to regulate plant tolerance to Zn deficiency. The effect of suboptimal Zn supply on the GSNOR enzyme and the effect of GSNOR overproduction on Zn uptake and Zn deficiency tolerance have not yet been examined. Therefore, this study aims to characterize the bidirectional relationship between GSNO/NO metabolism and Zn deficiency in the *Arabidopsis thaliana* model.

2. Materials and methods

2.1. Plant material and growing conditions

Wild type *Arabidopsis thaliana* L. (Columbia-0, Col-0) and GSNOR overproducer *35S::FLAG-GSNOR1* (Frungillo et al., 2014, kindly provided by Dr. Christian Lindermayr) were used during the experiments. The Arabidopsis seeds were subjected to surface sterilization using a solution containing 70% (v/v) ethanol and 5% (v/v) sodium hypochlorite. After this step, the seeds were transferred to a half-strength MS medium containing 1% sucrose (w/v) and 0.8% sucrose (w/v) agar. To minimize zinc contamination, the microbiological agar was washed three times overnight with 10 mM ethylenediaminetetraacetic acid (EDTA) solution (pH 7.5), followed by four washes with ultrapure water. The first wash was overnight, and the subsequent three washes were for 20 min each to remove EDTA (Bernal et al., 2012; Sinclair and Kramer, 2020). The seedlings were grown in media with 15 μM $ZnSO_4$ (control or full Zn), 1.5 μM $ZnSO_4$ (Zn/10) and 0 μM $ZnSO_4$ (Zn0) for 7 days. The Petri dishes were placed vertically in a greenhouse and maintained under controlled conditions (a photon flux density of 150 μmol $m^{-2} s^{-1}$, a 12/12 h light and dark cycle, a relative humidity of 45–55% and a temperature of 25 ± 2 °C). This closed and controlled system provided uniform growth of the plant material.

2.2. Analysis of Zn content by inductively coupled plasma mass spectrometry

The roots and shoots of *Arabidopsis thaliana* were harvested separately and dried at 70 °C for 24 h. 100 mg of dried plant material were processed using microwave-assisted acid digestion (MarsXpress CEM, Matthews, USA) in closed PTFE vessels at 200 °C and 1600 W with trace analytical quality nitric acid (6 mL, 65% w/v, Reanal, Hungary) and hydrogen peroxide (2 mL, 30% w/v, VWR Chemicals, Hungary) for 2 h. The analysis of the zinc content of the resulting solutions was done on a quadrupole Agilent 7700X (Santa Clara, USA) inductively coupled plasma mass spectrometer (ICP-MS) equipped with the standard Agilent integrated sample introduction system. The instrumental parameters employed were the following: 1550 W plasma forward power, 15.0 L/min plasma gas flow rate, 1.05 L/min carrier gas flow rate, 10.0 mm plasma sampling depth, 1 s integration time, 600 μl/min sample uptake rate. Determinations were carried out by recording signals at the ^{66}Zn isotope, using helium collision cell technology to eliminate any potential polyatomic interferences. Instrumental tuning was performed before all measurements using Agilent's tuning solutions (No. G1820–60,410). The zinc concentration for both organs is reported as μg/g values g/g based on dry weight (DW).

2.3. Analysis of NO- and Zn-associated gene expression by quantitative real-time PCR

Wild-type and *35S::FLAG-GSNOR1* seedlings (100 mg) were frozen in liquid nitrogen and stored at −80 °C. The gene expression level of *NON-SYMBIOTIC HEMOGLOBIN 1* (*GLB1*) (At2g16060), *NON-SYMBIOTIC HEMOGLOBIN 2* (*GLB2*) (At3g10520), *S-NITROSOGLUTATHIONE REDUCTASE 1* (*GSNOR1*) (At5g43940), *ZRT-/IRT-LIKE PROTEIN 3* (*ZIP3*) (At2g32270), *IRON-REGULATED TRANSPORTER 3* (*IRT3*) (At1g60960), *BASIC LEUCINE ZIPPER 19* (*bZIP19*) (At4g35040), *COPPER/ZINC SUPEROXIDE DISMUTASE 2* (*CSD2*) (At2g28190), *CARBONIC ANHYDRASE 2* (*CA2*) (At5g14740) were determined by quantitative real-time reverse transcription PCR (RT-qPCR). RNA was purified using the Quick-RNA Miniprep Kit (Zymo Research, Irvine, CA, USA) according to the manufacturer's instructions. NCBI primer design tools were used to design primers (Ye et al., 2012). The primer sequences are listed in Table S1. The NO and Zn-associated gene expression rate was detected by a quantitative real-time PCR machine (qTOWER 2.0, Jena Instruments). The PCR mixture contained 2 μL cDNA, 0.42 μL forward and reverse primers, 7 μL Maxima SYBR Green qPCR MasterMix (2 ×) (Thermo Fisher Scientific) and 4.16 μL nuclease-free water. The total volume of the RT-qPCR reaction was 14 μL. For amplification, a standard two-step thermal cycling profile was used (10 s at 95 °C and 1 min at 60 °C) for up to 40 cycles after a 15 min preheating step at 95 °C. Finally, a dissociation stage was added at 95 °C for 15 s, 60 °C for 15 s and 95 °C for 15 s. Data were analyzed using qPCRsoft 3.2 software (Jena Instruments). *The ACTIN2* (At3918780) and *GLYCERALDEHYDE-3-PHOSPHATE DEHYDROGENASE* 2 (*GAPDH2*) (At1913440) genes were used as references (Papdi et al., 2008). The expression data were calculated by the $2^{(-\Delta\Delta Ct)}$ formula. These measurements were carried out in three separate generations of plants with three technical replicates for each ($n = 3$).

2.4. Analysis of GSNOR activity by UV–vis absorption spectroscopy

The GSNOR activity was determined by monitoring NADH oxidation in the presence of GSNO at 340 nm (Sakamoto et al., 2002) using a KONTRON Uvikon double beam spectrophotometer. Fresh plant material (250 mg) was ground with extraction puffer (100 mM TRIS-HCl (pH 7.5), 10% (m/v) glycerol, 0.2% (m/v) Triton-X, 2 mM DTT and 0.1 mM EDTA). The homogenate was centrifuged at 9300 × *g* for 20 min at 4 °C. 150 μL of protein extract was incubated in 650 μL reaction buffer (20 mM TRIS–HCl pH 8.0, 0.5 mM EDTA), 100 μL 0.2 mM NADH and 100 μL 0.4 mM GSNO. Protein concentration was measured with the Bradford protein assay (Bradford, 1976). Data are expressed as nanomoles of NADH/min/mg protein. The measurement of GSNOR activity was performed in three separate generations of plants with three technical replicates in each ($n = 3$).

2.5. Determination of RNS and ROS levels by fluorescence microscopy

Semiquantitative determination of NO levels in root tips was performed with 10 μM 4-amino-5-methylamino-2′,7′-difluorofluorescein diacetate (DAF-FM DA) fluorescent probe. The staining solution was prepared in 10 mM TRIS-HCl buffer (pH 7.4). The samples were incubated for 30 min in darkness at room temperature, then the samples were washed two times with buffer and placed on microscopic slides (Kolbert et al., 2012).

Dihidrorhodamine 123 (DHR, 10 μM) was used to detect peroxynitrite levels at the root tips. Samples were incubated with the probe for 15 min at room temperature in darkness and washed twice with 5 mM TRIS-HCl buffer (pH 7.4) before microscopic analysis (Kolbert et al., 2012).

The whole seedlings were immersed in 50 μM 10-acetyl-3,7 dihydroxyphenoxazine (Amplex Red) prepared in 50 mM sodium phosphate buffer (pH 7.5) to label H_2O_2 levels. After 30 min of incubation at room

temperature in darkness, the seedlings were washed in 50 mM sodium phosphate buffer (pH 7.5) and placed on microscopic slides (Lehotai et al., 2012).

2.6. Analysis of GSNOR protein amount and protein tyrosine nitration by western blot

For protein extraction, 50 mM TRIS-HCl extraction buffer (pH 7.6–7.8) was used to grind Arabidopsis seedlings. Protein extract was centrifuged at 4 °C, 9300 × *g* for 20 min and treated with 1% proteinase inhibitor, stored at −20 °C. Protein concentrations were measured using bovine serum albumin as a standard (Bradford, 1976).

15 μL of denaturated protein was subjected to SDS-PAGE on a 12% acrylamide gel. Proteins were transferred to PVDF membranes using the wet blotting procedure (25 mA, 16 h). Membranes were used for cross-activity assays with rabbit polyclonal antibody (anti-GSNOR, Agrisera, cat. No. AS09 647) against GSNOR (Sigma-Aldrich, cat. No. N0409, 1: 2000 diluted). The loading controls were performed using anti-actin antibody (Agrisera, Cat. No. AS13 2640) and as protein standard actin (bovine muscle, Sigma-Aldrich, cat. No. A3653) was used.

In case of protein tyrosine nitration, a rabbit polyclonal antibody against 3-nitrotyrosine (1:2000) was used. Immunodetection was performed using affinity isolated goat anti-rabbit IgG alkaline phosphatase secondary antibody (Sigma-Aldrich, Cat. No. A3687, 1: 10,000) at a dilution of 1: 10,000, and the bands were visualized using the NBT/BCIP (5-bromo-4-chloro-3-indolyl phosphate) reaction. As a positive control, nitrated bovine serum albumin (NO_2-BSA) (Sigma-Aldrich, cat No. A3653) was used. Protein bands were quantified using Gelquant software (provided by biochemlabsolutions.com) and expressed as pixel densities. Western blot was performed on three separate protein extracts from independent plant generations, at least twice per extract (Kolbert et al., 2018).

2.7. Analysis of in planta zinc ion levels and cell viability by fluorescence microscopy

Whole seedlings of Col-0 and *35::FLAG-GSNOR1* Arabidopsis seedlings were washed three times with 10 mM EDTA before adding a 20 μM Zinpyr-1 solution in 10 mM phosphate buffered saline (PBS; 137 mM NaCl, 2.68 mM KCl, 8.1 mM Na_2HPO_4, 1.41 mM KH_2PO_4, pH 7.4). Samples were incubated in probe solution in darkness for 3 h at room temperature (Sinclair et al., 2007). Zinpyr-1 labelled samples were mounted in PBS and images were taken with a Leica TCS SP5 confocal laser scanning microscope using excitation at 488 nm with a 100 mW Ar ion laser, 10 × and 20 × objective with fluorescein isothiocyanate (FITC) filter. Images were analysed using Fiji software (http://fiji.sc/Fiji; Schindelin et al., 2012). These detections were performed three times with 10 samples each ($n = 30$).

For time-dependent detection of Zn ion levels in Arabidopsis root tips, the ethyl (2-methyl-8-p-toluenesulfonamide-6-quinolyloxy) acetate probe (Zinquin) was used according to Helmersson et al. (2008). The seedlings were equilibrated in PBS and further incubated in a 25 μM Zinquin solution (in PBS) for 60 min at room temperature in darkness. Before microscopic investigation, the samples were washed once with PBS buffer. An epifluorescent microscope was used for the detection of Zinquin-related fluorescence.

The viability of the root meristem cells was detected using fluorescein diacetate (FDA). Arabidopsis seedlings were incubated in 10 μM dye solution for 30 min, in darkness, at room temperature and washed two times with 10 mM TRIS-HCl buffer (pH 7.4) according to Kolbert et al. (2012). The epifluorescence microscope was used for the detection of fluorescein-related fluorescence.

2.8. Epifluorescence microscopy

Epifluorescence analyzes were performed using an Axiovert 200 M fluorescence microscope (Carl Zeiss, Jena, Germany) equipped with a digital camera (Axiocam HR). Filter set 10 (exc.: 450–490, em.: 515–565 nm) was used for DAF-FM, FDA, and DHR. Filter set 20 (exc.: ~540, em.: ~590 nm) for the Amplex Red and DAPI filter set (exc.: 365, em.: 455/50 nm) for Zinquin. The intensity of the pixels was measured in the roots in the circles. These analyzes were carried out at least three times with 10 root tips examined ($n = 10$).

2.9. Statistical analysis

All results are expressed as mean ± SE. Graphs were prepared in Microsoft Excel 2016 and SigmaPlot 12. For statistical analysis, the Tukey test (one-way ANOVA, $P < 0.05$) was used in SigmaPlot 12.

3. Results and discussion

3.1. Limited zinc supply results in reduced zinc ion content of Arabidopsis seedlings: organ and tissue levels

The Zn content in both organs of healthy plants was similar (~200–250 μg/g DW), indicating that Zn is homogeneously distributed between the bottom and above organs of Arabidopsis. In the root system of Col-0 and *35S::FLAG-GSNOR1 Arabidopsis thaliana* seedlings, the decrease rate of Zn content was dependent on the amount of Zn in the nutrient medium. For example, in the Col-0 roots, the Zn content decreased by 68% and 83% compared to the control (full Zn) in case of Zn/10 and Zn0 treatments, respectively (Table 1). The tendency and extent of Zn ion depletion as an effect of limited Zn supply was similar in the shoot system (decreases by 67% and 76% in Col-0 plants treated with Zn/10 and Zn0, respectively). For most plant species, a decrease in the Zn content of the shoot below 15–20 μg/g DW indicates Zn deficiency (Marschner, 2012; Noulas et al., 2018). The measured Zn concentration (~40 μg/g DW, Table 1) in the shoot system of *A. thaliana* reflects that either reducing the amount of added Zn or withdrawing it did not result in Zn deficiency, but caused a significant decrease of *in planta* Zn content during the 7-day treatment period. The transgenic line showed no difference compared to Col-0, since Zn limitation caused a decrease in Zn content of a similar magnitude and tendency (eg, 63% and 83% decrease in the roots of plants treated with Zn/10 and Zn0, respectively) (Table 1). This means that our hypothesis was not confirmed, since GSNOR overproduction does not influence Zn uptake under Zn limited conditions.

The Zn-specific fluorescence probe showed that in the primary root meristem of the optimally Zn-supplied *35S::FLAG-GSNOR1*, the Zn level was lower than that of Col-0 (Figs. 1A, B). Significantly reduced Zn-associated fluorescence signal was measured compared to control in Col-0 Arabidopsis grown in nutrient medium with mild Zn deficiency (Fig. 1A, B). Additionally, total Zn withdrawal caused a significant decrease in fluorescence (58%) at the Col-0 root tip, but the rate of Zn decrease was milder compared to the Zn/10 treatment. In the GSNOR overproducing line, the Zn level did not decrease significantly in the case of Zn/10 or Zn0 conditions (Fig. 1A, B). This indicates that a slight difference between the Zn levels of the two lines can be detected at the

Table 1
Zinc ion concentrations (μg/g dry weight, DW) of wild-type (Col-0) and *35S::FLAG-GSNOR1 Arabidopsis thaliana* grown on agar medium with 15 μM $ZnSO_4$ (full Zn), 1.5 μM $ZnSO_4$ (Zn/10) and 0 μM $ZnSO_4$ (Zn0) for 7 days.

	root $[Zn^{2+}]$ μg/g DW	shoot $[Zn^{2+}]$ μg/g DW
Col-0 full Zn	258.22 ± 3.82	184.74 ± 0.51
Col-0 Zn/10	84.33 ± 0.69	62.96 ± 0.76
Col-0 Zn0	43.23 ± 0.19	44.37 ± 0.37
***35S::FLAG-GSNOR1* full Zn**	220.66 ± 1.76	249.65 ± 4.47
***35S::FLAG-GSNOR1* Zn/10**	81.97 ± 1.05	73.76 ± 1.16
***35S::FLAG-GSNOR1* Zn0**	39.37 ± 0.63	43.94 ± 0.51

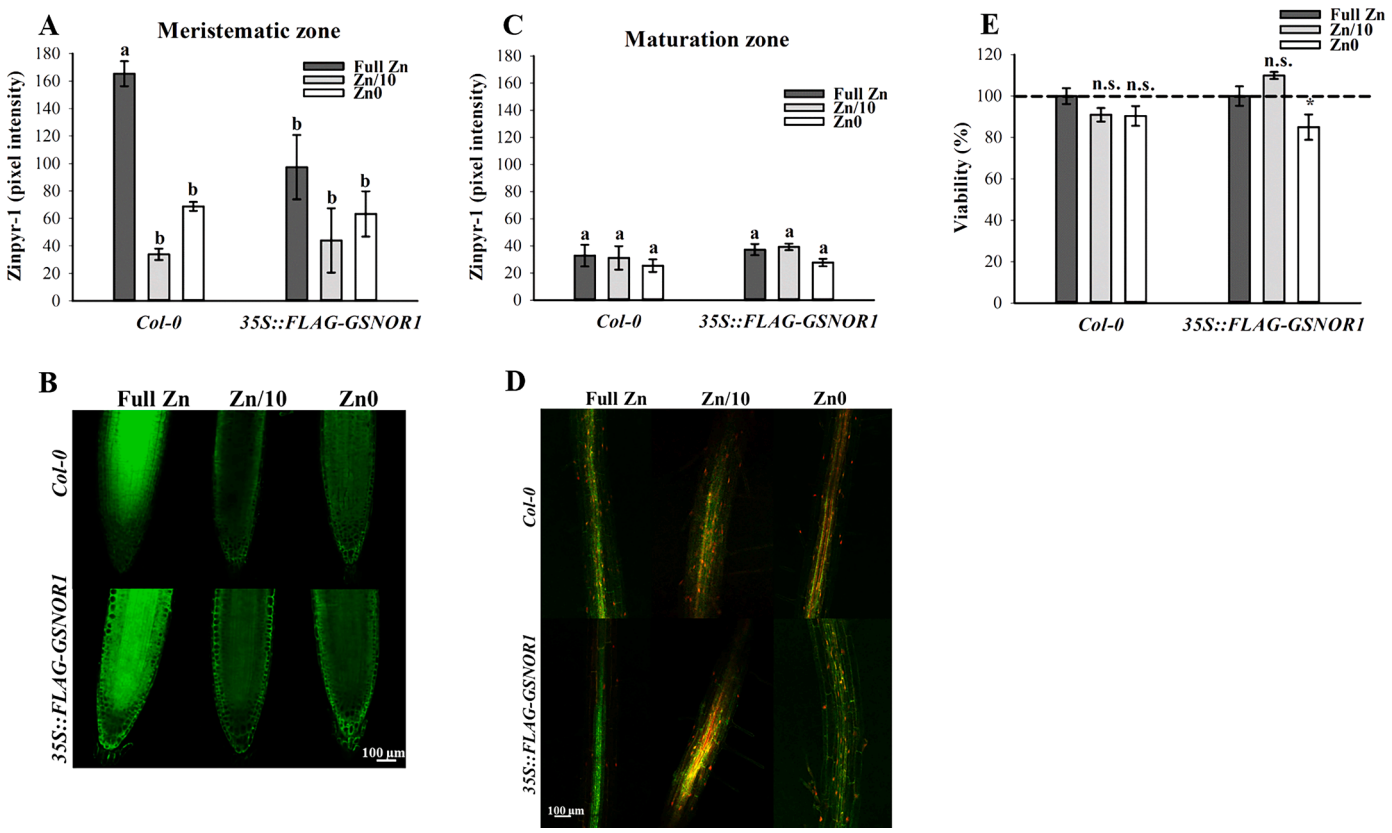

Fig. 1. Fluorescence intensity of Zinpyr-1 probe indicating *in situ* Zn ion levels in the meristematic (A) and maturation (C) zones of the primary root of wild-type (Col-0) and *35S::FLAG-GSNOR1 Arabidopsis thaliana* grown on agar media with 15 µM $ZnSO_4$ (Full Zn), 1.5 µM $ZnSO_4$ (Zn/10) and 0 µM $ZnSO_4$ (Zn0) for 7 days. Different letters indicate significant differences according to Tukey test ($n = 10$, $p \leq 0.05$). Representative fluorescent microscopic images of Zinpyr-1 labelled root tips (B) and upper root parts (D). Scale bars=100 µm. (E) Viability (control%) of the root meristem cells in Col-0 and *35S::FLAG-GSNOR1* plants. Significant differences were indicated by asterisks according to Student's *t*-test ($n = 10$, $^*P \leq 0.05$). n.s.=non-significant.

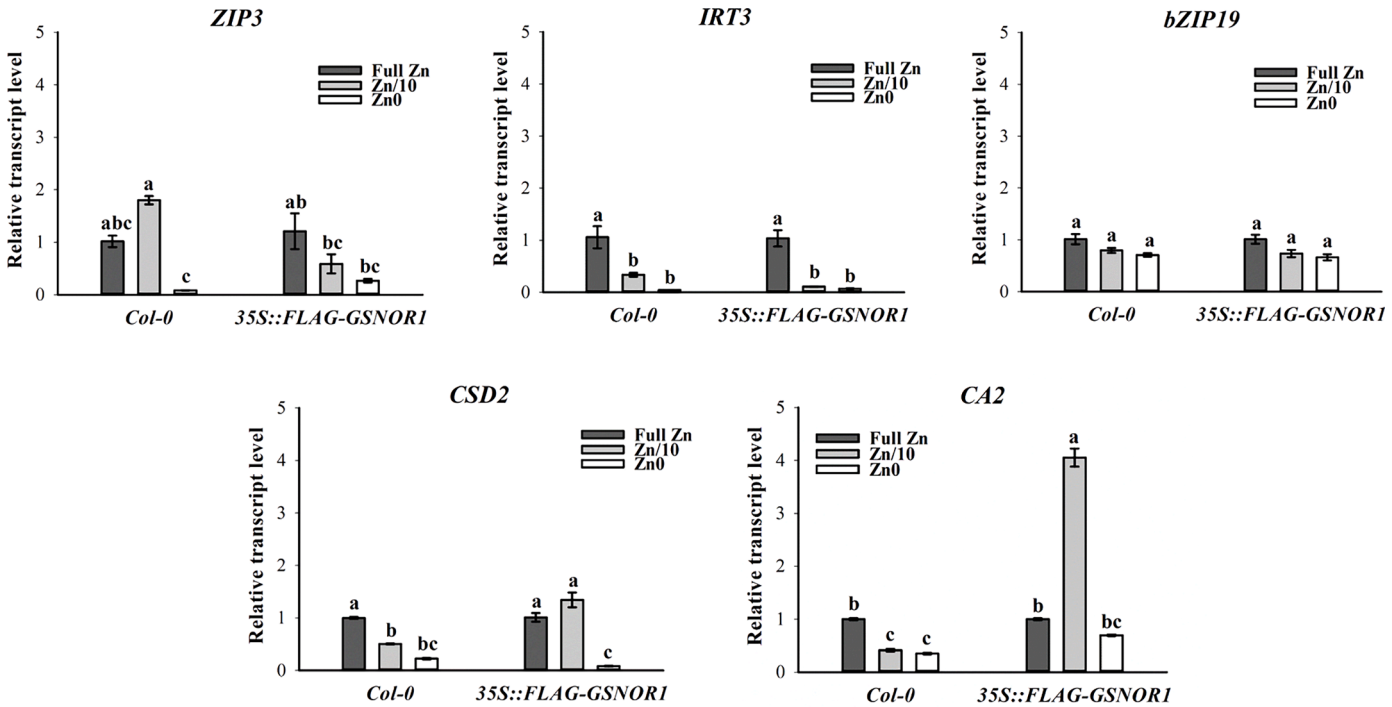

Fig. 2. Relative transcript levels of Zn-deficiency marker genes in wild-type (Col-0) and *35S::FLAG-GSNOR1 Arabidopsis thaliana* grown on agar media with 15 µM $ZnSO_4$ (Full Zn), 1.5 µM $ZnSO_4$ (Zn/10) and 0 µM $ZnSO_4$ (Zn0) for 7 days. Different letters indicate significant differences according to Tukey test ($n = 3$, $p \leq 0.05$).

tissue level (with a higher resolution), but this difference does not appear when measured in the whole seedlings suggesting the need for studying the effect of Zn limitation at multiple levels. In the upper root regions, the Zn-specific fluorescent staining could not detect the decreased Zn level in neither plant line grown in the case of limited Zn supply (Figs. 1C, D).

As a function of time, the Zn level of the Col-0 root showed significant fluctuations at all rates of Zn supply (Fig. S 1). On the fourth and seventh days after treatment, the difference was the largest in the Zn levels of the plants grown in the full Zn medium and the plants with limited Zn supply (Fig S 1). Reduced Zn levels did not cause loss of cell viability in Col-0, while a slight decrease was observed in the GSNOR overproducer line as a result of complete withdrawal of Zn (Fig. 1E). Overall, although Zn limitation resulted in decreased Zn concentration of the seedlings, it did not cause Zn deficiency and did not lead to a significant decrease in cell viability in any of the lines. We did not observe differences in the tolerance to Zn limitation between the Col-0 and GSNOR overproducer line, which is contrary to the responses observed during other nutrient stresses such as excess Zn or inhibiting nitrate doses (Kolbert et al., 2019; Frungillo et al., 2014).

3.2. Zinc deprivation influences the expression of Zn deficiency marker genes in A. thaliana seedlings

Among Zn-deficiency marker genes, the *ZIP3* transporter transcript level did not change in response to mild Zn deficiency in Col-0, while it decreased to around 0 in response to complete Zn deprivation (Fig. 2). In *35S::FLAG-GSNOR1, ZIP3* expression was not significantly modified by Zn/10 or Zn0 treatments. The expression of the other Zn transporter, *IRT3*, was significantly reduced as a result of both Zn limitations in both species (Fig. 2). In contrast to these, Campos et al. (2017) reported induced expression of *ZIP3* and *IRT3* in Zn-deficient Arabidopsis. The expression of the *bZIP19* transcription factor showed unchanged levels compared to the control in the case of both treatments in both lines (Fig. 2). As its activity is directly controlled posttranscriptionally by Zn status, *AtbZIP19* expression is not or only slightly upregulated upon Zn deficiency in Arabidopsis (Lilay et al., 2021). The genes of the two Zn-requiring marker enzymes *CSD2* and *CA2* showed similar Zn limitation-induced changes. Both degrees of Zn deprivation decreased the expression of the *CSD2* and *CA2* genes in Col-0. Interestingly, mild Zn deprivation caused a 4-fold increase in *CA2* expression of the transgenic line (Fig. 2).

In this experimental system, among the marker genes, the expression of the enzyme genes and the transcription factor gene showed changes that were consistent with the literature. The different response of the *ZIP3* and *IRT*3 transporter genes to the limitation of Zn may be due to the fact that Arabidopsis plants possessed a reduced tissue Zn level, but were not actually Zn deficient (see Table 1). Additionally, *IRT3* is not specific to Zn; therefore, its expression could be modified by other factors (mainly iron levels).

3.3. Zn limitation influences GSNOR expression and protein abundance, but does not modify enzyme activity

The GSNOR enzyme requires Zn ions for its catalytic activity, and therefore, it is assumed that the reduced Zn supply may affect the enzyme. In Col-0, a slight but significant decrease in *GSNOR1* transcript level compared to the control occurred due to Zn/10 treatment, but the difference was not significant in the case of more severe Zn deprivation (Zn/0) (Fig. 3A). Regarding the amount of GSNOR protein, both degrees of Zn limitation notably reduced it in Col-0 (Fig. 3B). In the case of the *35S::FLAG-GSNOR1* line, the reduced Zn supply did not cause changes in *GSNOR1* expression (Fig. 3A) and protein amount (Fig. 3B and S 2), due to the possibility that overproduction compensates for the negative effect of Zn deficiency. At the same time, it is also conceivable that the possible changes could not be detected due to the oversaturation of the

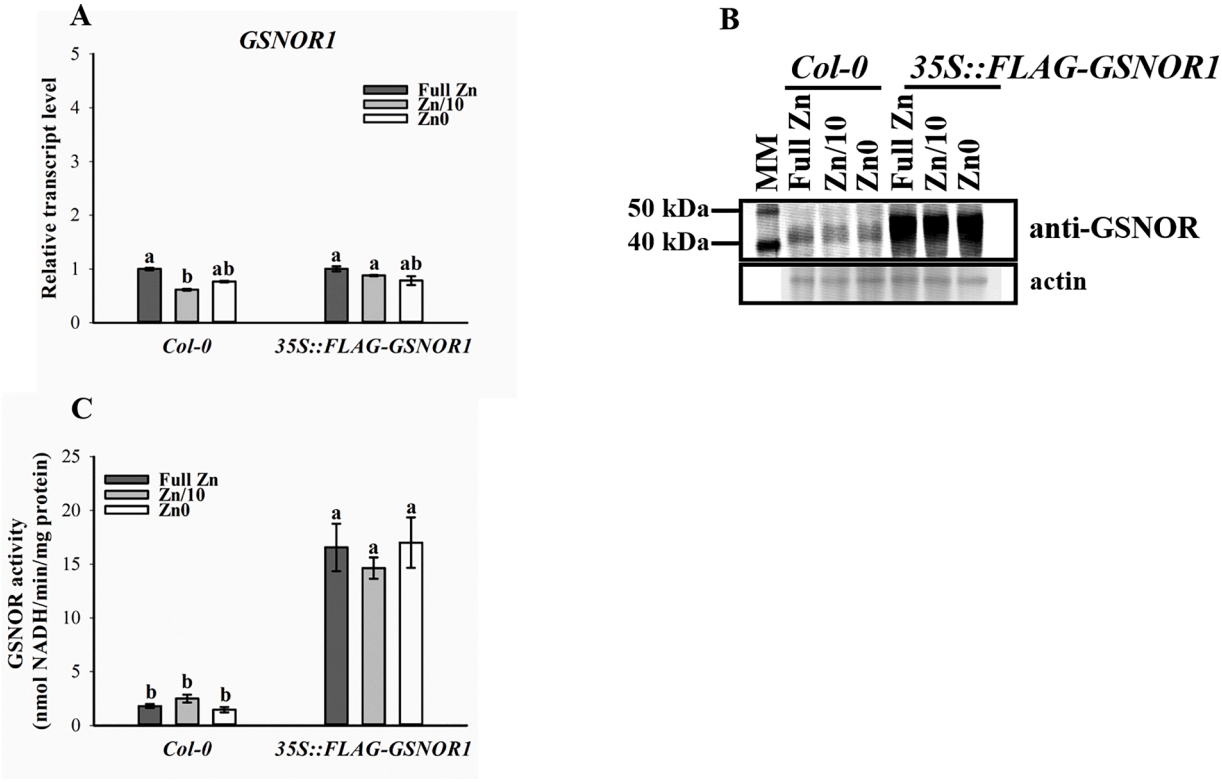

Fig. 3. Relative transcript level of *AtGSNOR1* gene (A), protein abundance (B) and specific activity (C) of GSNOR in wild-type (Col-0) and *35S::FLAG-GSNOR1 Arabidopsis thaliana* grown on agar media with 15 μM $ZnSO_4$ (Full Zn), 1.5 μM $ZnSO_4$ (Zn/10) and 0 μM $ZnSO_4$ (Zn0) for 7 days. Different letters indicate significant differences according to Tukey test ($n = 3$, $p \leq 0.05$). For the western blot, anti-actin was used as a loading control. MM= molecule marker.

western blot membrane (Fig. 3B). Interestingly, a suboptimal Zn-induced decrease in GSNOR activity was not detected in any of the treatments, in any of the lines (Fig. 3C). These reflect that the expression and protein amount of GSNOR are influenced by inadequate Zn supply, but these changes do not manifest themselves in altered enzyme activity. These suggest that –against our hypothesis- limited Zn availability does not influence the function of the GSNOR enzyme despite its Zn requirement. In contrast, GSNOR activity is generally induced by abiotic stresses, including iron deficiency (Romera et al., 2023). It can be suspected that in our system plants suffered only mild stress, the extent of which was not sufficient to induce changes in GSNOR activity.

3.4. Suboptimal Zn supply induces an increase in NO, $ONOO^-$ and H_2O_2 levels and intensifies protein tyrosine nitration

In Col-0, the mild limitation of Zn triggered an increase in the NO level, while in the case of Zn0 treatment, the NO level of the roots was similar to the full Zn condition (Fig. 4A, F). The reason for the increase in the NO level induced by Zn limitation is not the inactivation of GSNOR (Fig 3C), but it can be the activation of synthesis pathways (eg, nitrate reductase, polyamines). These possibilities need further examination. Furthermore, the Zn limitation did not induce significant changes in the expressions of *GLB1* and *GLB2* (Figs 4B, C) therefore, their contribution to the increase in NO level is negligible. Examining NO levels as a function of time, we found that the fluctuation was relatively large in both control and Zn-limited plants (Fig. S 3). On the fourth and seventh days of treatment, the difference between the NO levels of the Zn-

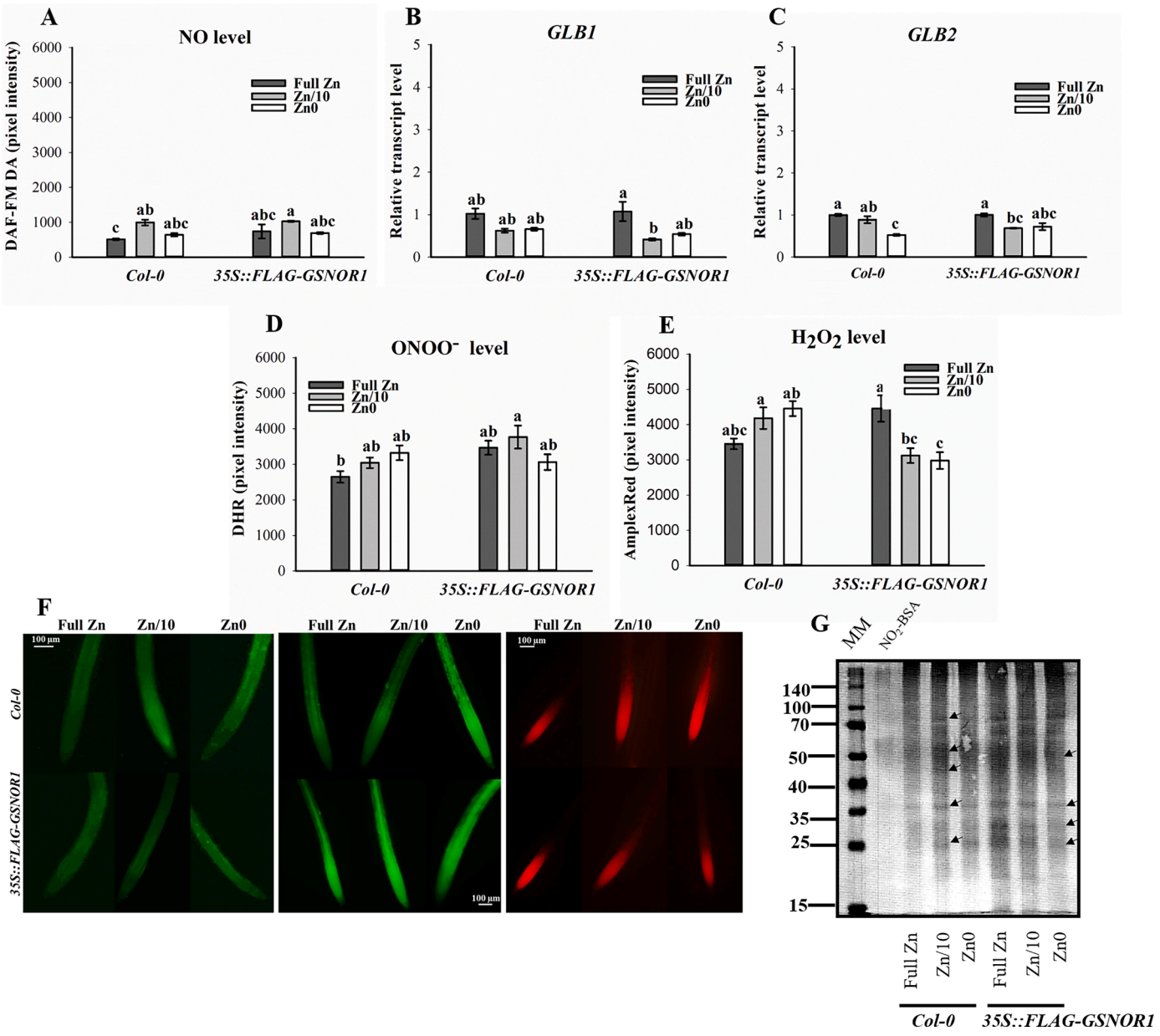

Fig. 4. The level of NO (A), $ONOO^-$ (D) and H_2O_2 (E) in the root tips of wild-type (Col-0) and *35S::FLAG-GSNOR1 Arabidopsis thaliana* grown on agar media with 15 µM $ZnSO_4$ (Full Zn), 1.5 µM $ZnSO_4$ (Zn/10) and 0 µM $ZnSO_4$ (Zn0) for 7 days. Relative transcript level of *GLB1* (B) and *GLB2* (C) genes. Different letters indicate significant differences according to Tukey test ($n = 10$, $p \leq 0.05$). (F) Representative fluorescence microscopic images of DAF-FM DA- (for NO), DHR123- (for $ONOO^-$) or Amplex Red- (for H_2O_2) labelled root tips. Scale bars= 100 µm. (G) Representative western blot membrane indicating protein tyrosine nitration. MM= molecule marker, NO_2-BSA= nitrated bovine serum albumin. Black arrows indicate protein bands with modifying nitration signal.

starved and control plants was the greatest (Fig. S 3). The Zn level showed the same tendency, because it was the lowest due to the Zn limitation on the fourth and seventh days compared to the control (Fig. S 1). The similar time courses of suboptimal Zn-triggered changes of NO and Zn levels in the roots of *A. thaliana* suggest their association. In Col-0, $ONOO^-$ levels showed a concentration-dependent but statistically nonsignificant increase, while unaffected $ONOO^-$levels were detected in the GSNOR overproducer line (Fig. 4D, F). On the contrary, the H_2O_2 level increased in Col-0 (statistically nonsignificant) depending on the level of Zn limitation, while it decreased significantly in *35S::FLAG-GSNOR1* compared to control as an effect of Zn deprivation (Fig. 4E, F). These suggest that the high expression / amount of proteins / activity of GSNOR prevents suboptimal Zn-induced H_2O_2 formation and thus may moderate oxidative stress. This hypothesis is supported by the recent paper by Li et al. (2021), where GSNOR is considered a master regulator of oxidative stress responses in plants.

In healthy individuals from both Arabidopsis lines, *3*-nitrotyrosine was detected in numerous protein bands suggesting the existence of a physiological nitroproteome (Fig 4G, Kolbert et al., 2017; Corpas et al., 2021). It should be noted that the extent of protein nitration was higher in the GSNOR overproducer line compared to Col-0 (Fig. 4G and Fig. S 4). The basal $ONOO^-$ and H_2O_2 levels were higher (not statistically significant) in *35S::FLAG-GSNOR1* supplied optimally with Zn than in Col-0 (Figs. 4D, E, F), which may be associated with the elevated rate of physiological protein nitration. Additionally, we suggest that GSNOR overproduction down-regulates SNO signaling, thereby altering the balance between protein nitration and *S*-nitrosation and shifting it towards nitration. In Col-0, both degrees of limited Zn supply increased the amount of *3*-nitrotyrosine in proteins (intensified signal in at least five protein bands compared to the control, indicated by arrows in Fig. 4G, Fig. S4 A), which may be associated with the Zn deprivation-induced elevation of $ONOO^-$ and H_2O_2 levels (Fig. 4D, E, F). Similar to this, Zn limitation resulted in intensified tyrosine nitration in *Brassica napus* (Molnár et al., 2022); therefore, we may suggest that suboptimal Zn supply has a pronitrant effect on the plant proteome, possibly causing functional loss and proteasomal degradation of target proteins (Kolbert and Lindermayr, 2021). Interestingly, the level of tyrosine nitration decreased compared to the control in at least four protein bands in *35S::FLAG-GSNOR1* grown in the presence of suboptimal Zn levels (indicated by arrows in Fig. 4G and Fig. S4 B) reflecting the influence role of GSNOR overproduction on protein tyrosine nitration. This suggests an indirect interaction between NO-dependent PTMs.

4. Conclusion

Comparison of Col-0 and *35S::FLAG-GSNOR1* Arabidopsis shows that GSNOR overproduction does not have an effect on the Zn limitation-induced reduction of *in planta* Zn content. Moreover, the Zn level of the root apex is responsive to the Zn content of the nutrient medium, and the Zn-sensitive fluorescent probe provides a rapid, *in situ,* noninvasive tool for the detection of Zn deficiency in plants. Suboptimal Zn supply results in a smaller but more active GSNOR protein pool in Col-0 *A. thaliana*. Contrary to our expectations, the plant maintains its GSNOR activity; thus, the SNO levels and signaling may be controlled in plants with reduced Zn content. In *35S::FLAG-GSNOR1,* the overproduction possibly compensates the negative effects of reduced Zn supply, resulting in unchanged GSNOR expression, protein abundance and activity. Suboptimal Zn supply alters NO levels but does not significantly modify $ONOO^-$ and H_2O_2 levels and exerts a pronitrant effect on the plant proteome that may cause functional loss of target proteins. Overall, this is the first report to prove that limited Zn supply inhibits the GSNOR enzyme at gene and protein levels but not at the activity level, slightly induces NO levels, and increases physiological nitroproteome in Arabidopsis. The results contribute to complementing existing information on the molecular mechanisms of Zn deficiency by revealing the effects on NO signaling.

Declaration of Competing Interest

The authors declare that they have no known competing financial interests or personal relationships that could have appeared to influence the work reported in this paper.

Data availability

Data will be made available on request.

Acknowledgments

This work was supported by the National Research, Development and Innovation Office (K135303). Supported by the NKP-22–3-SZTE-437 New National Excellence Program of the Ministry of Culture And Innovation the National Research, Development, and Innovation Fund. The *35S::FLAG-GSNOR1* seeds were kindly provided by Dr. Christian Lindermayr (Helmholtz Centrum, Munich). The authors thank Éva Kapásné Török and Erzsébet Porkoláb for their help during the experimental work.

Supplementary materials

Supplementary material associated with this article can be found, in the online version, at doi:10.1016/j.stress.2023.100250.

References

Alloway, B.J., 2008. Micronutrient Deficiencies in Global Crop Production, first ed. Springer, Dordrecht.
Bradford, M., 1976. A rapid and sensitive method for the quantification of microgram quantities of protein utilizing the principle of protein-dye binding. Anal. Biochem. 72, 23422–23426.
Bernal, M., Casero, D., Singh, V., et al., 2012. Transcriptome sequencing identifies SPL7-regulated copper acquisition genes FRO4/FRO5 and the copper dependence of iron homeostasis in Arabidopsis. Plant Cell 24, 738–761.
Cakmak, I., 2000. Possible roles of zinc in protecting plant cells from damage by reactive oxygen species. New Phytol. 146, 185–205.
Campos, A.C.A.L., Kruijer, W., Alexander, R., Akkers, R.C., Danku, J., Salt, D.E., Aarts, M. G.M., 2017. Natural variation in Arabidopsis thaliana reveals shoot ionome, biomass, and gene expression changes as biomarkers for zinc deficiency tolerance. J. Exp. Bot. 68, 3643–3656.
Corpas, F.J., Alché, J.D., Barroso, J.B., 2013. Current overview of S-nitrosoglutathione (GSNO) in higher plants. Front. Plant Sci. 4, 126. https://doi.org/10.3389/fpls.2013.00126.
Corpas, F.J., González-Gordo, S., Palma, J.M., 2021. Protein nitration: A connecting bridge between nitric oxide (NO) and plant stress. Plant Stress 2, 100026. https://doi.org/10.1016/j.stress.2021.100026.
Das, S., Green, A., Fan, M.X., 2019. Zinc deficiency in Indian soils is associated with low crop productivity and crop quality. Better Crops–South Asia 11, 11–14.
Frungillo, L., Skelly, M.J., Loake, G.J., Spoel, S.H., Salgado, I., 2014. S-nitrosothiols regulate nitric oxide production and storage in plants through the nitrogen assimilation pathway. Nat. Comm. 5, 1–10.
Gow, A.J., Farkouh, C.R., Munson, D.A., Posencheg, M.A., Ischiropoulos, H., 2004. Biological significance of nitric oxide-mediated protein modifications. Am. J. Physiol. Lung Cell. Mol. Physiol. 287, L262–L268.
Helmersson, A., von Arnold, S., Bozhkov, P.V., 2008. The level of free intracellular zinc mediates programmed cell death/cell survival decisions in plant embryos. Plant Physiol. 147, 1158–1167.
Jahnová, J., Luhová, L., Petřivalský, M., 2019. S-nitrosoglutathione reductase—The master regulator of protein S-nitrosation in plant NO signaling. Plants 8, 48. https://doi.org/10.3390/plants8020048.
Kolbert, Zs., Pető, A., Lehotai, N., Feigl, G., Ördög, A., Erdei, L., 2012. In vivo and in vitro studies on fluorophore-specificity. Acta Biol. Szeged. 56, 37–41.
Kolbert, Zs., Feigl, G., Bordé, Á., Molnár, Á., Erdei, L., 2017. Protein tyrosine nitration in plants: Present knowledge, computational prediction and future perspectives. Plant Physiol. Biochem. 113, 56–63.
Kolbert, Zs., Lindermayr, C., 2021. Computational prediction of NO-dependent posttranslational modifications in plants: current status and perspectives. Plant Physiol. Biochem. 167, 851–861.
Kolbert, Zs., Molnár, Á., Szőllősi, R., Feigl, G., Erdei, L., Ördög, A., 2018. Nitro-oxidative stress correlates with Se tolerance of Astragalus species. Plant Cell Physiol. 59, 1827–1843.
Kolbert, Zs., Molnár, Á., Oláh, D., Feigl, G., Horváth, E., Erdei, L., Lindermayr, C., 2019. S-Nitrosothiol signaling is involved in regulating hydrogen peroxide metabolism of zinc-stressed Arabidopsis. Plant Cell Physiol. 60, 2449–2463.

Kondak, S., Molnár, Á., Oláh, D., Kolbert, Zs., 2022. The role of nitric oxide (NO) in plant responses to disturbed zinc homeostasis. Plant Stress 4, 100068. https://doi.org/10.1016/j.stress.2022.100068.

Lehotai, N., Kolbert, Z., Pető, A., et al., 2012. Selenite-induced hormonal and signalling mechanisms during root growth of Arabidopsis thaliana L. J. Exp. Bot. 63, 5677–5687.

Li, B., Sun, C., Lin, X., Busch, W., 2021. The emerging role of GSNOR in oxidative stress regulation. Trend. Plant Sci. 26, 156–168.

Lilay, G.H., Persson, D.P., Castro, P.H., et al., 2021. Arabidopsis bZIP19 and bZIP23 act as zinc sensors to control plant zinc status. Nat. Plants 7, 137–143. https://doi.org/10.1038/s41477-021-00856-7.

Lindermayr, C., 2018. Crosstalk between reactive oxygen species and nitric oxide in plants: key role of S-nitrosoglutathione reductase. Free Rad. Biol. Med. 122, 110–115.

Marschner, P., 2012. Marschner's Mineral Nutrition of Higher Plants, third ed. Academic Press. https://doi.org/10.1016/C2009-0-63043-9.

Molnár, A., Kondak, S., Benkő, P., et al., 2022. Limited Zn supply affects nutrient distribution, carbon metabolism and causes nitro-oxidative stress in sensitive Brassica napus. Environ. Exp. Bot. 202, 105032 https://doi.org/10.1016/j.envexpbot.2022.105032.

Natasha, N., Shahid, M., Bibi, I., et al., 2022. Zinc in soil-plant-human system: A data-analysis review. Sci. Total Environ. 808, 152024 https://doi.org/10.1016/j.scitotenv.2021.152024.

Noulas, C., Tziouvalekas, M., Karyotis, T., 2018. Zinc in soils, water and food crops. J. Trace Elem. Med. Biol. 49, 252–260.

Papdi, C., Ábrahám, E., Joseph, M.P., Popescu, C., Koncz, C., Szabados, L., 2008. Functional identification of Arabidopsis stress regulatory genes using the controlled cDNA overexpression system. Plant Physiol. 147, 528–542.

Romera, F.J., García, M.J., Lucena, C., Angulo, M., Pérez-Vicente, R., 2023. RNO is not the same as GSNO in the regulation of Fe deficiency responses by dicot plants. Int. J. Mol. Sci. 24, 12617. https://doi.org/10.3390/ijms241612617.

Sakamoto, A., Ueda, M., Morikawa, H., 2002. Arabidopsis glutathione-dependent formaldehyde dehydrogenase is an S-nitrosoglutathione reductase. FEBS Lett. 515, 20–24.

Schindelin, J., Arganda-Carreras, I., Frise, E., et al., 2012. Fiji: an open-source platform for biological-image analysis. Nat. Method. 9, 676–682.

Sinclair, S.A., Sherson, S.M., Jarvis, R., Camakaris, J., Cobbett, C.S., 2007. The use of the zinc-fluorophore, Zinpyr-1 in the study of zinc homeostasis in Arabidopsis roots. New Phytol. 174, 39–45.

Sinclair, S.A., Krämer, U., 2020. Generation of effective zinc-deficient agar-solidified media allows identification of root morphology changes in response to zinc limitation. Plant Signal. Behav. 15, 1687175 https://doi.org/10.1080/15592324.2019.1687175.

Szabó, C., Ischiropoulos, H., Radi, R., 2007. Peroxynitrite: biochemistry, pathophysiology and development of therapeutics. Nat. Rev. Drug Discover. 6, 662–680.

Ye, J., Coulouris, G., Zaretskaya, I., Cutcutache, I., Rozen, S., Madden, T.L., 2012. Primer-BLAST: a tool to design target-specific primers for polymerase chain reaction. BMC Bioinfo. 13, 1–11.